

Supplementary Information

Seasonality

In Figure S1, we present plots analogous to Figure 1.b in the main text, calculated for four representative months: January, representing winter and corresponding to the period when the COVID-19 outbreak started; April, representing spring; July, for the summer period ; and October representing autumn.

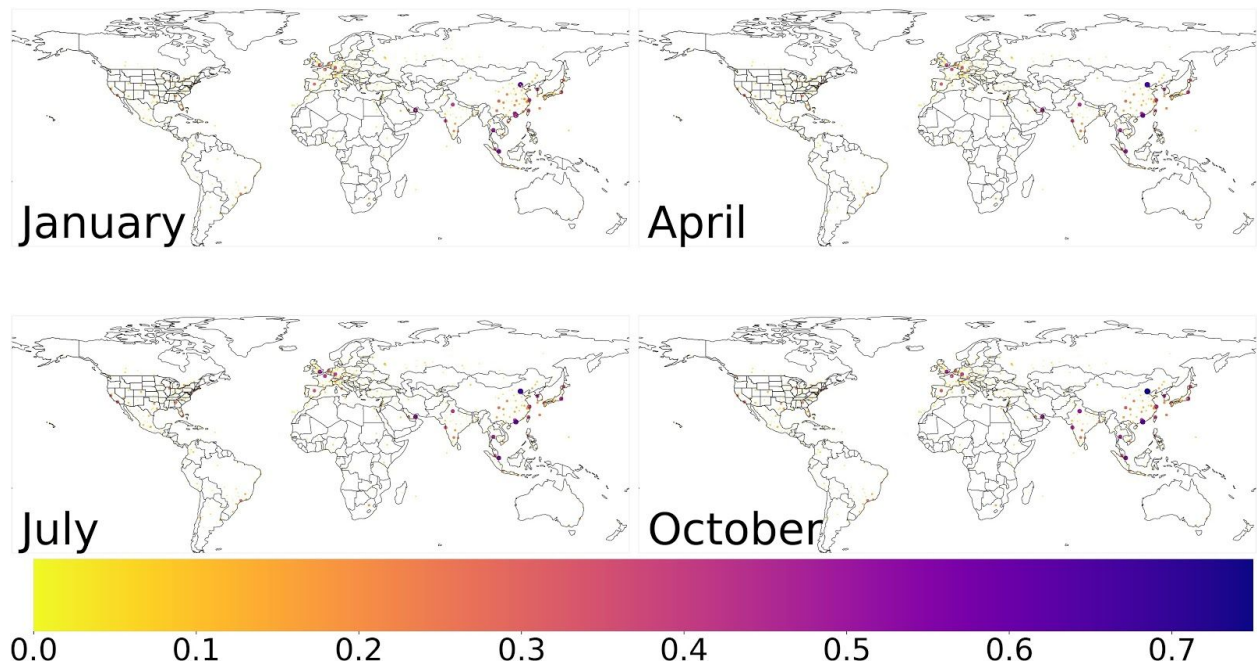


Figure S1: Risk measure for different months. Note that for visualization purposes, the color scale is truncated to [0,0.75]. Circle area is proportional to risk.

Infectious period

We analysed different values of the shape parameter κ of the gamma distribution of the infectious period (see Methods in the main text) The second was done for different values of R .

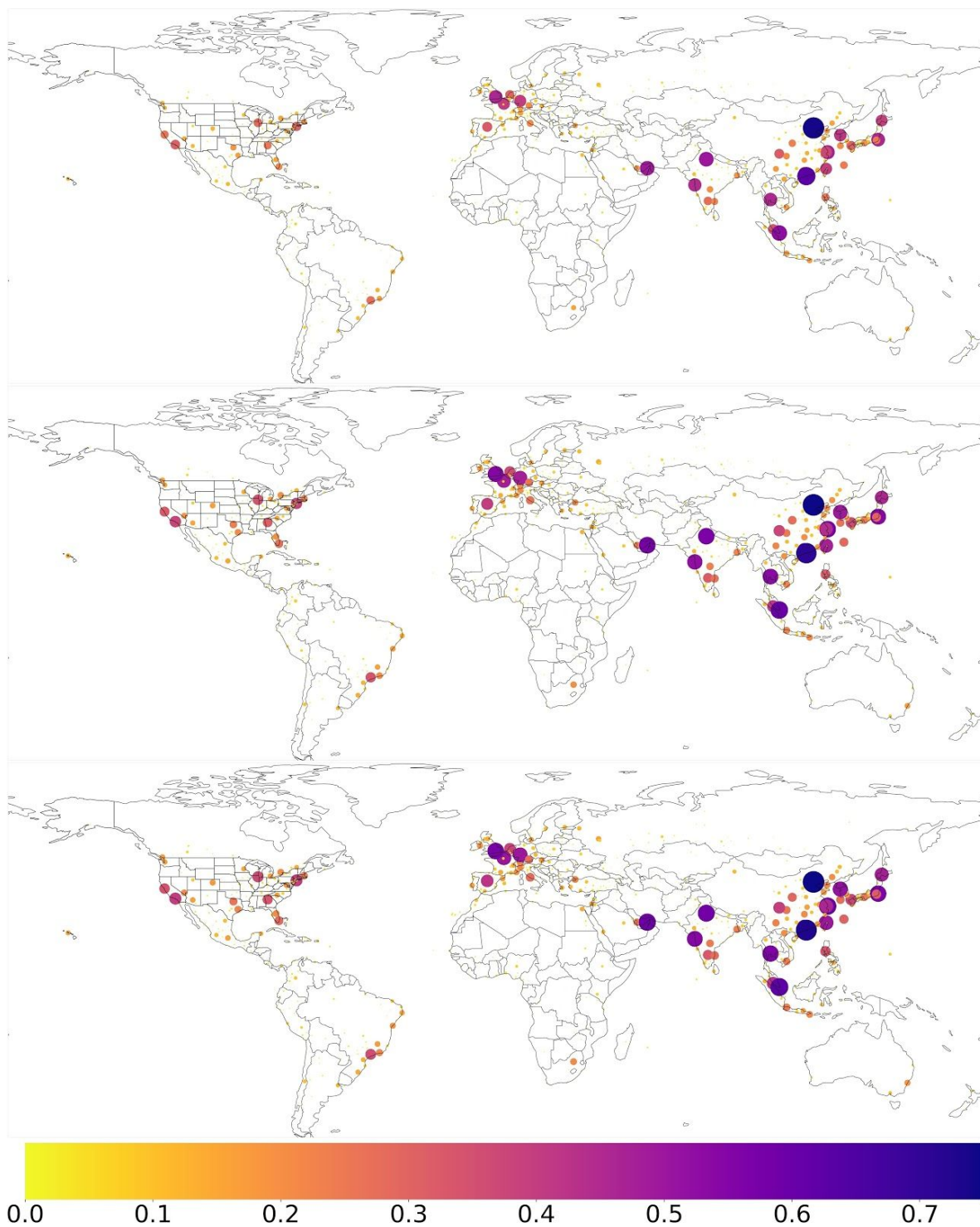


Figure S2: Risk measure for (top to bottom) $\kappa = 1, 3, 6$. Compare to Figure 1.b from the main text. Note that for visualization purposes, the color scale is truncated to $[0, 0.75]$. Circle area is proportional to risk.

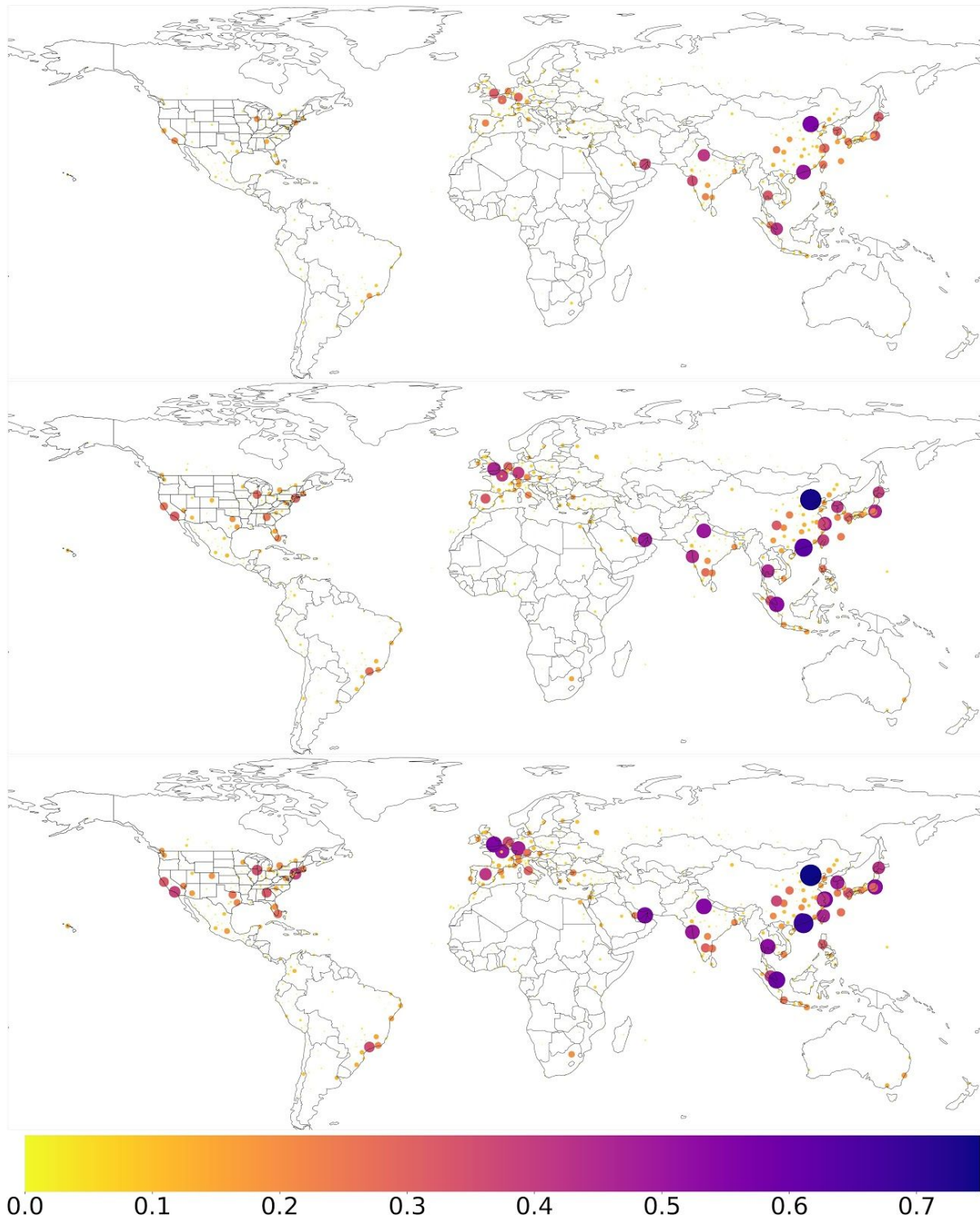


Figure S3: Risk measure for (top to bottom) $R_0 = 2, 3, 4$. Compare to Figure 1.b from the main text. Note that for visualization purposes, the color scale is truncated to $[0, 0.75]$. Circle area is proportional to risk.

Superspreaders

Extending the calculation performed in [1] , we can calculate the probability of an outbreak from superspreaders by defining α as the fraction of superspreaders; $\beta^{(1)}, \beta^{(2)}$ as the transmission coefficients of superspreaders and non-superspreaders, respectively; and q_{ij} as the probability of not causing sustained transmission from i superspreaders and j non-superspreaders. Hence

$$q_{1,0} = \alpha\beta^{(1)}/(\beta^{(1)} + \gamma)q_{1,0}^2 + (1 - \alpha)\beta^{(1)}/(\beta^{(1)} + \gamma)q_{1,0}q_{0,1} + \gamma/(\beta^{(1)} + \gamma)$$

$$q_{0,1} = \alpha\beta^{(2)}/(\beta^{(2)} + \gamma)q_{1,0}q_{0,1} + (1 - \alpha)\beta^{(2)}/(\beta^{(2)} + \gamma)q_{0,1}^2 + \gamma/(\beta^{(2)} + \gamma)$$

Finally, $\alpha q_{1,0} + (1 - \alpha)q_{0,1}$ provides the probability of not causing an outbreak in case of superspreaders. We explore this scenario with $\alpha = 0.01, \beta^{(1)}/\beta^{(2)} = 5, \gamma = 7, \beta^{(2)} = R\gamma$ for $R = 3$ below. Varying parameter values produced similar results.

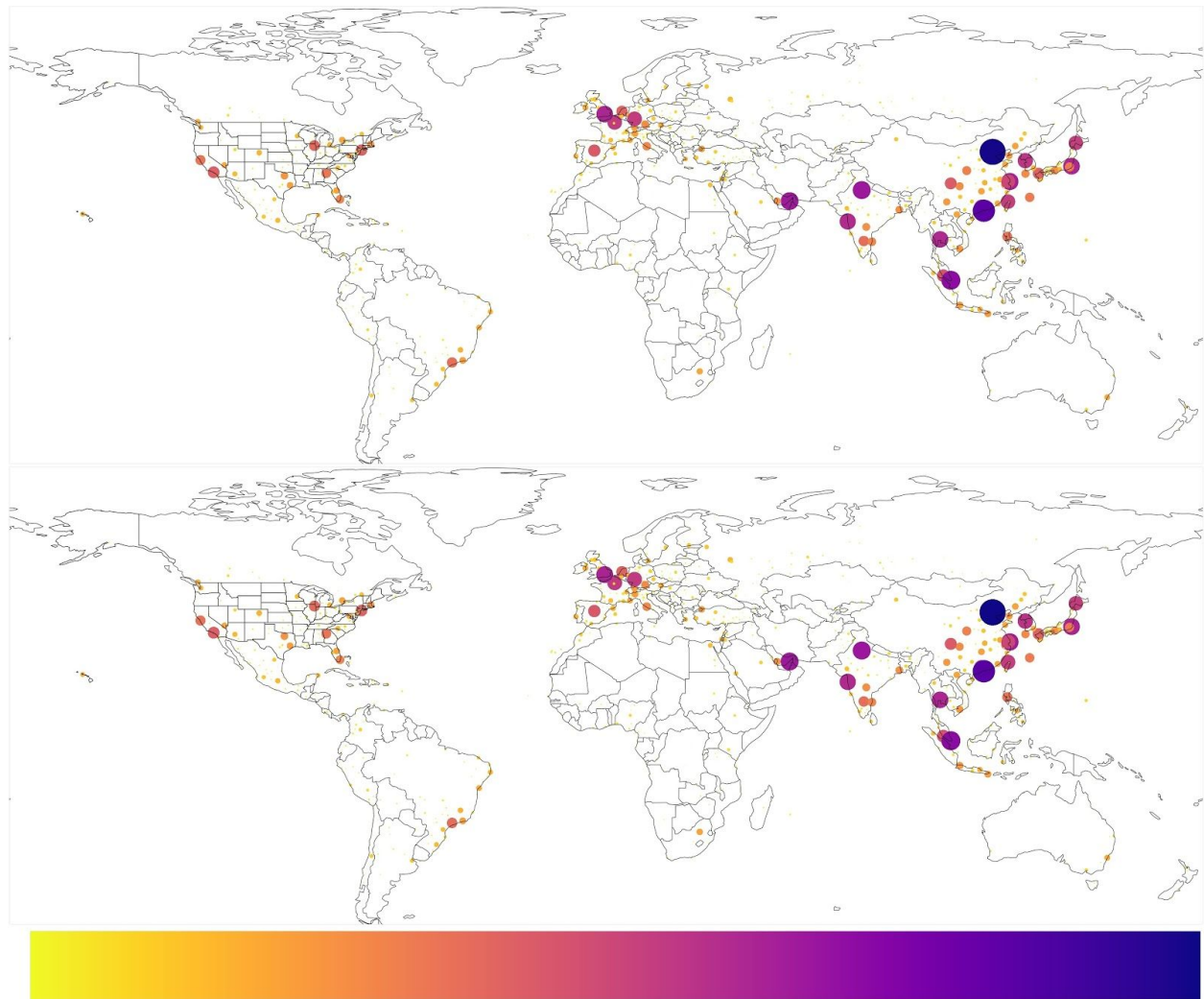


Figure S4: Risk measure with (bottom) and without (top) superspreaders. Compare to Figure 1.b from the main text. Note that for visualization purposes, the color scale is truncated to $[0,0.75]$. Circle area is proportional to risk.

Outbreak risk by airport

Below we show the probability of an outbreak caused by introducing one infected individual landing at a specific airport.

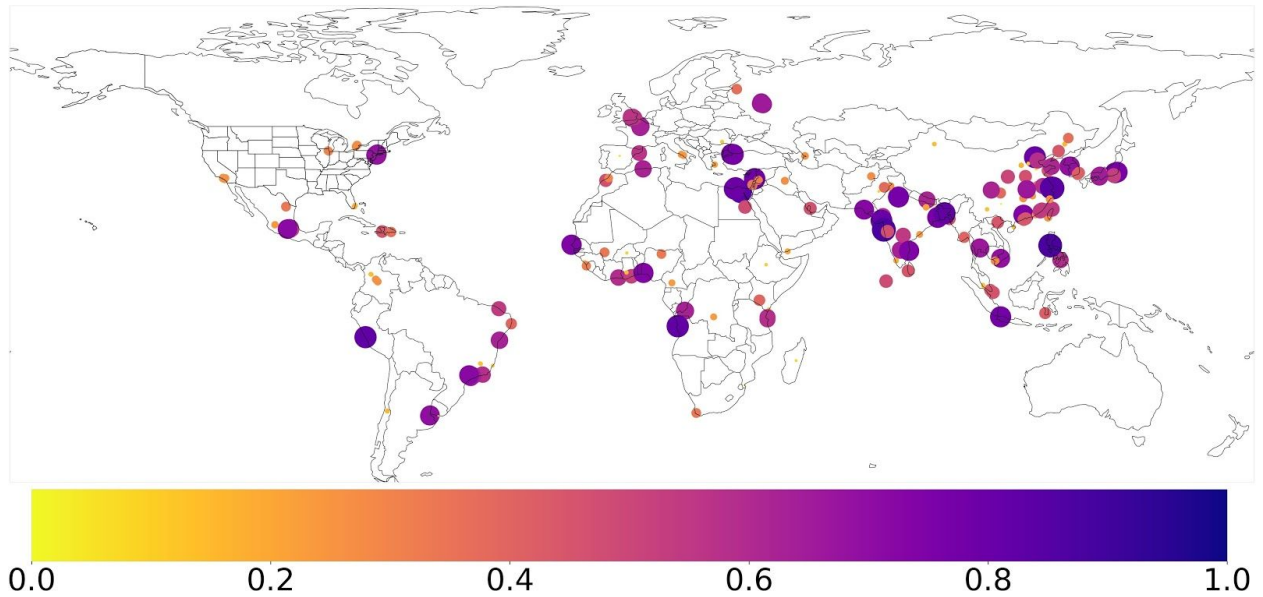


Figure S5: Likelihood of initiating an outbreak by introducing one infected individual in a city. Many of the cities most susceptible to outbreaks are in India and China. Circle area is proportional to risk.

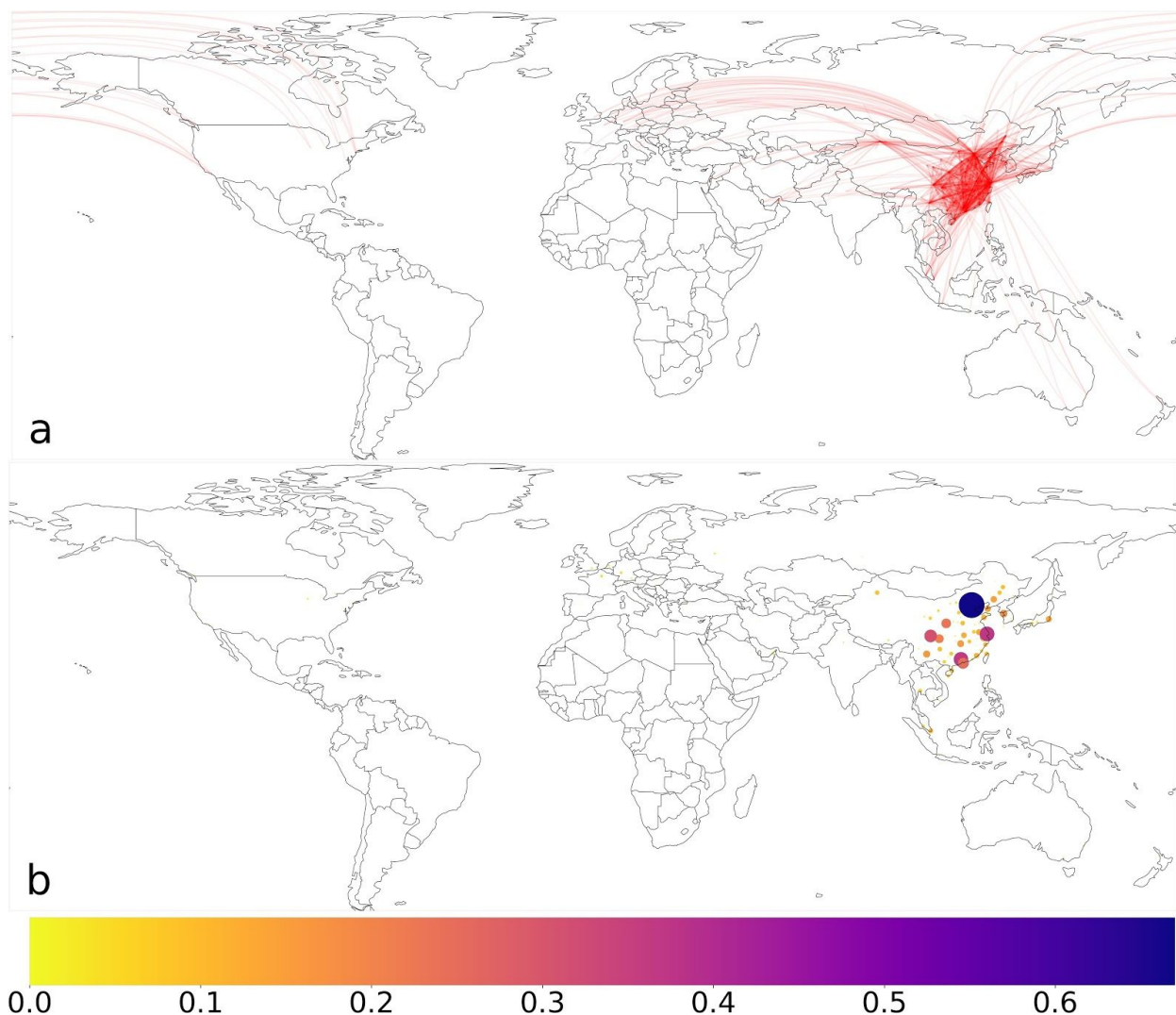


Figure S6: Airport connectivity and risk of outbreak initiation in China. a) A global map, overlaid with connections between global airports to an airport in China (red). Each connection represents the amount of air travel between locations to an airport in China, to which the curve opacity is proportional. b) The probability of passengers from different airports to initiate a COVID-19 outbreak in China, represented by color and circle area. Note that for visualization purposes, the color scale is truncated to $[0, 0.67]$.

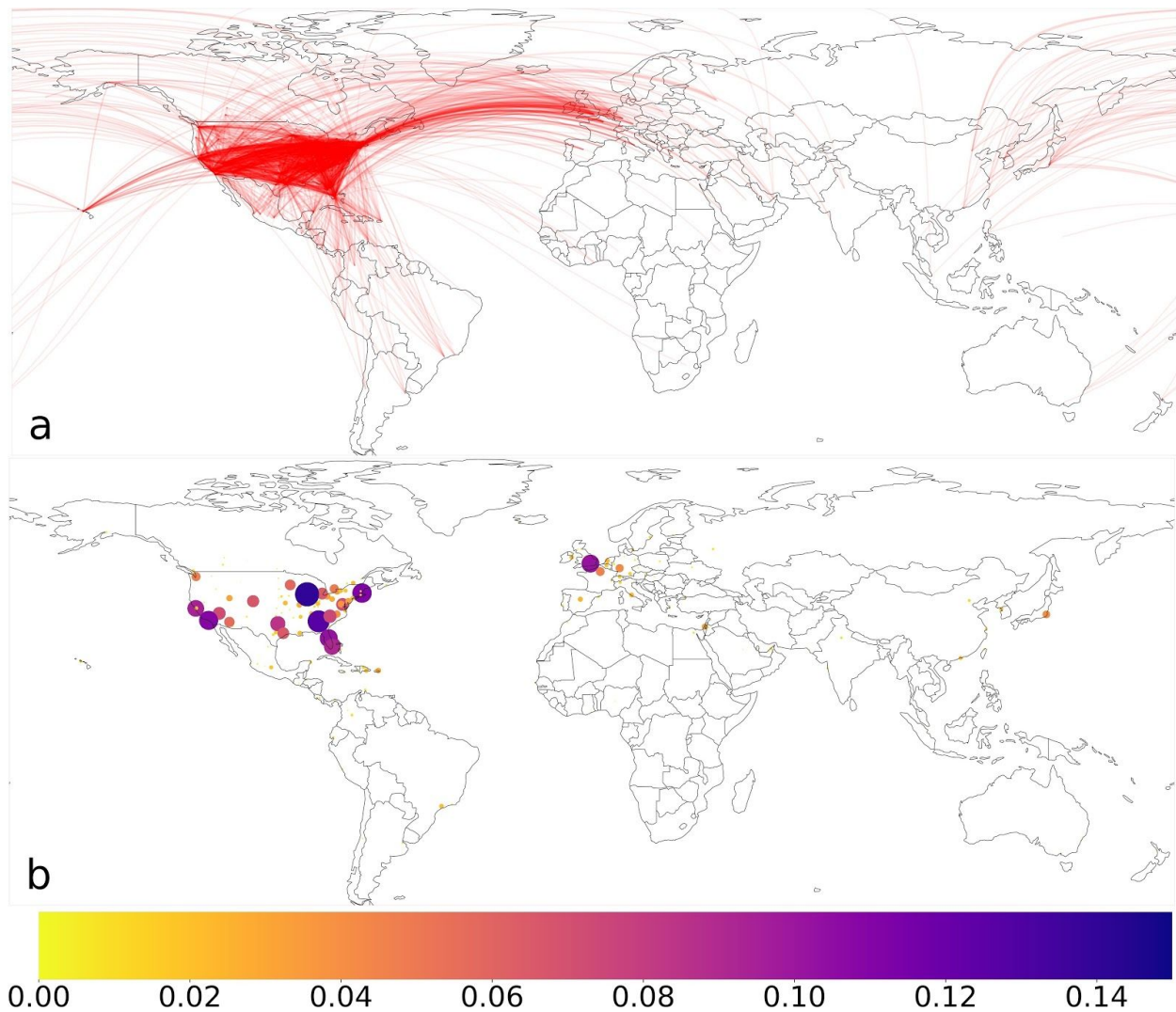


Figure S7: Airport connectivity and risk of outbreak initiation in the United States. a) A global map, overlaid with connections between global airports to an airport in the United States (red). Each connection represents the amount of air travel between locations to an airport in the United States, to which the curve opacity is proportional. b) The probability of passengers from different airports to initiate a COVID-19 outbreak in the United States, represented by color and circle area. Note that for visualization purposes, the color scale is truncated to $[0, 0.15]$.

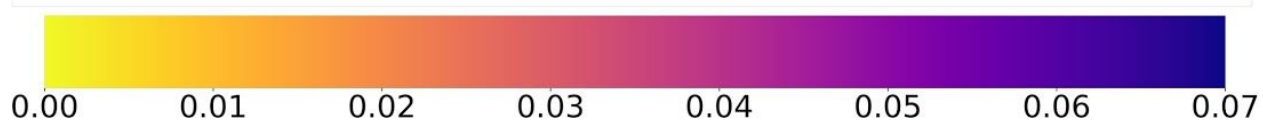
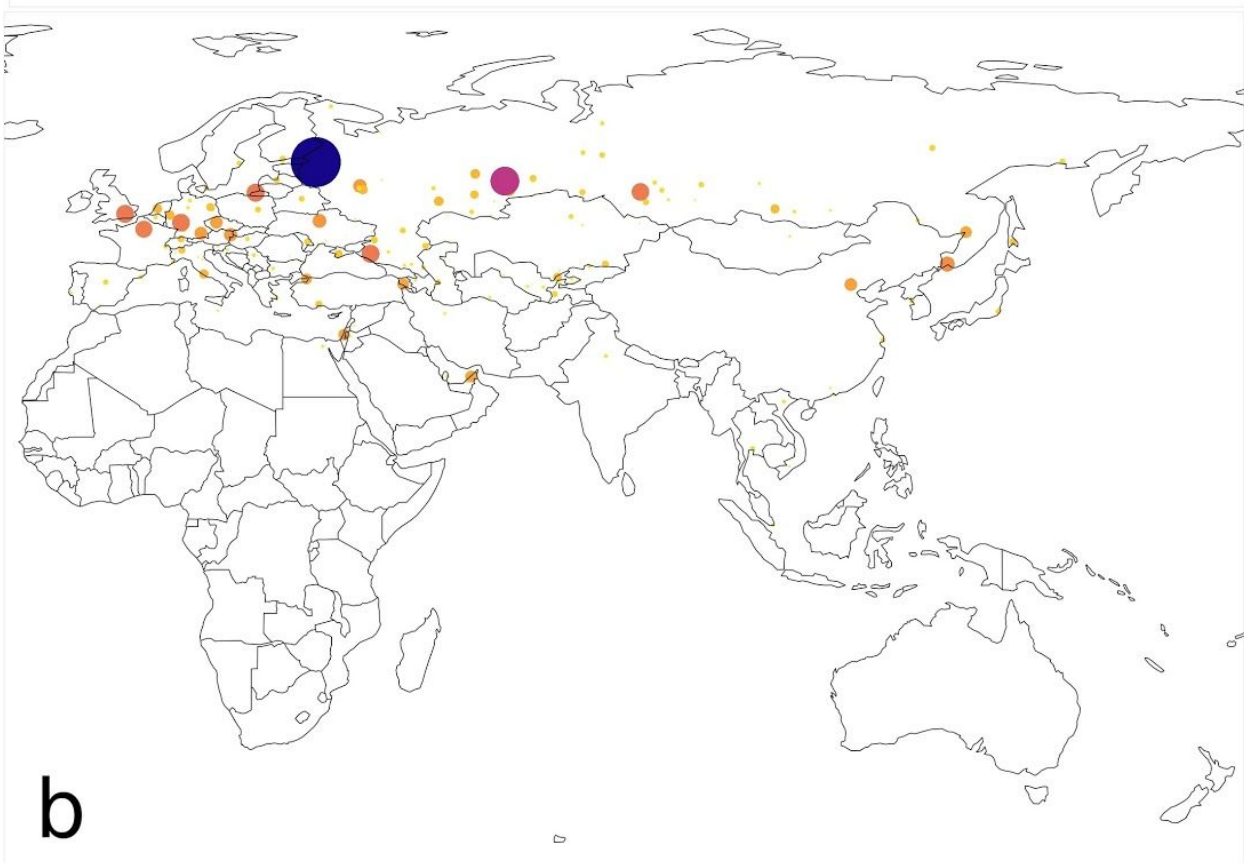
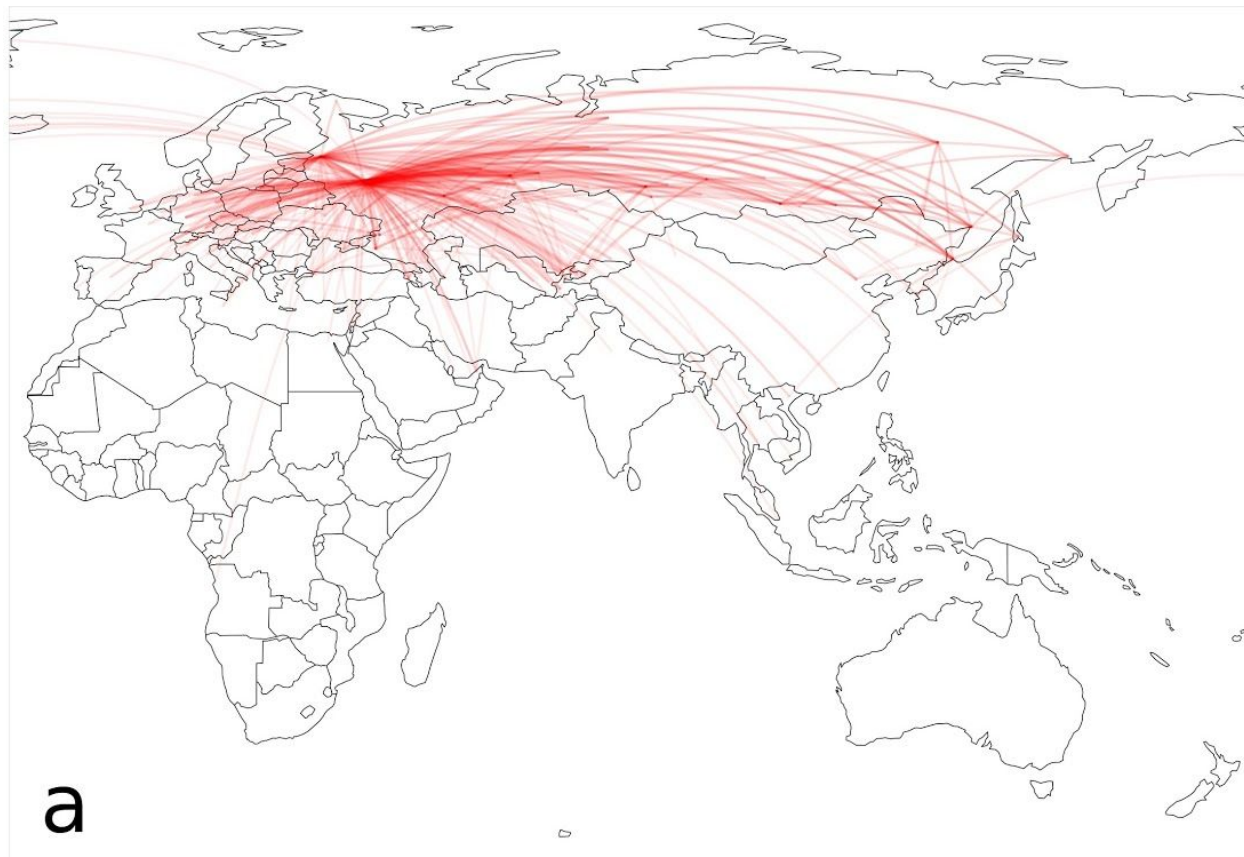


Figure S8: Airport connectivity and risk of outbreak initiation in Russia. a) A global map, overlaid with connections between global airports to an airport in Russia (red). Each connection represents the amount of air travel between locations to an airport in Russia, to which the curve opacity is proportional. b) The probability of passengers from different airports to initiate a COVID-19 outbreak in Russia, represented by color and circle area. Note that for visualization purposes, the color scale is truncated to [0,0.07].

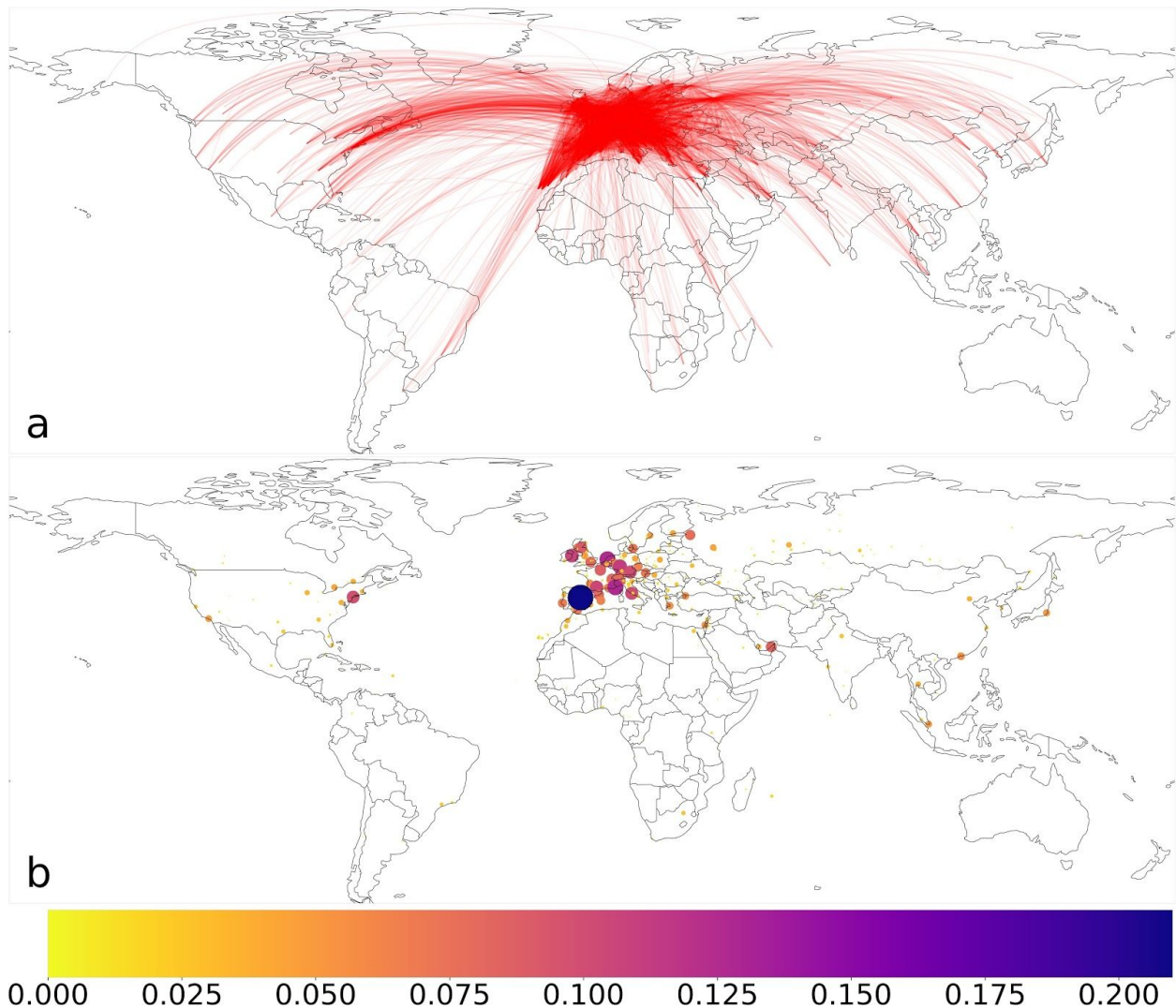


Figure S9: Airport connectivity and risk of outbreak initiation in Europe. a) A global map, overlaid with connections between global airports to an airport in Europe (red). Each connection represents the amount of air travel between locations to an airport in Europe, to which the curve opacity is proportional. b) The probability of passengers from different airports to initiate a COVID-19 outbreak in Europe, represented by color and circle area. Note that for visualization purposes, the color scale is truncated to [0,0.21].

Supplementary table S1: The risk of outbreak posed by each airport, along with some metadata (region, continent, etc.) extracted from [2].

Supplementary table S2: The risk of outbreak posed by introducing one infected individual at an airport, along with the calculated density and reproduction number estimated for each airport.

Supplementary table S3: The full table of risks. Includes origin and destination airport names, as well as the predicted traffic between them for the month of October, with lower and upper bounds, according to [3]. Column risk_i is the risk of an outbreak caused by passengers travelling from the origin airport, dest_p_no_outbreak is the probability that no outbreak at the destination is initiated by a passenger from the origin, and risk_ij is $1 - \text{dest_p_no_outbreak}$. The table also contains coordinates for the origin and destination, as well as other metadata.

References

- [1] R. N. Thompson, "Novel coronavirus outbreak in Wuhan, China, 2020: Intense surveillance Is vital for preventing sustained transmission in new locations," *J. Clin. Med.*, vol. 9, no. 2, p. 498, 2020.
- [2] "Ourairports.com. 2020.," *Ourairports*. <https://ourairports.com/> (accessed Apr. 10, 2020).
- [3] L. Mao, X. Wu, Z. Huang, and A. J. Tatem, "Modeling monthly flows of global air travel passengers: An open-access data resource," *J. Transp. Geogr.*, vol. 48, pp. 52–60, 2015.